



**HAL**  
open science

## Boundary Control for Multi-Directional Traffic on Urban Networks

Liudmila Tumash, Carlos Canudas de Wit, Maria Laura Delle Monache

► **To cite this version:**

Liudmila Tumash, Carlos Canudas de Wit, Maria Laura Delle Monache. Boundary Control for Multi-Directional Traffic on Urban Networks. 2021. hal-03182546v1

**HAL Id: hal-03182546**

**<https://hal.science/hal-03182546v1>**

Preprint submitted on 26 Mar 2021 (v1), last revised 24 Oct 2021 (v2)

**HAL** is a multi-disciplinary open access archive for the deposit and dissemination of scientific research documents, whether they are published or not. The documents may come from teaching and research institutions in France or abroad, or from public or private research centers.

L'archive ouverte pluridisciplinaire **HAL**, est destinée au dépôt et à la diffusion de documents scientifiques de niveau recherche, publiés ou non, émanant des établissements d'enseignement et de recherche français ou étrangers, des laboratoires publics ou privés.

# Boundary Control for Multi-Directional Traffic on Urban Networks

Liudmila Tumash, Carlos Canudas-de-Wit and Maria Laura Delle Monache

**Abstract**—This paper is devoted to the boundary control design for traffic evolving on large-scale urban networks. The state corresponds to the vehicle density that evolves on a continuum two-dimensional plane. This plane represents an urban network, whose parameters are interpolated as a function of distance to the physical roads. The dynamics of the vehicle density are governed by a newly developed multi-direction traffic flow model called the NSWE-model that encompasses a system of four coupled partial differential equations (PDEs). Each of these PDEs describes the density evolution in one of the four cardinal directions: North, South, West and East. For this model we design a control applied at the network’s upstream boundary to drive a multi-directional congested traffic state to a desired equilibrium state. We analyse the class of desired states the system can be driven to. Finally, the result is validated numerically using the real network of Grenoble downtown.

## I. INTRODUCTION

Ever growing urban areas face the problem of transportation efficiency drop during rush hours. This problem triggers challenges for researchers to develop realistic traffic models able to predict congestion formation, as well as to suggest efficient control measures able to improve the overall traffic throughput. The first attempts to model traffic on a macroscopic scale were made by Lighthill and Whitgham [3] and Richards [4] by introducing the kinematic wave theory. The LWR-model is a first-order hyperbolic PDE based on the conservation of vehicles that describes the propagation of traffic on one road as a fluid. Its key assumption is the existence of a concave relation between traffic flow and density known as Fundamental Diagram (FD).

The LWR framework was extended to networks with the introduction of intersection modelling in [10]. However, if a network consists of thousands of links and junctions, the computational cost of solving a Riemann problem at every intersection may become too high [9]. Thus, it was necessary to develop macroscopic approaches for traffic modelling. Using data from microsimulations, [6] revealed the existence of a relation between flow and density on a city level. This relation was then confirmed in a real experiment due to data collection from Yokohama, Japan [12], [11]. The discovery of macroscopic fundamental diagram (MFD) allowed to

describe traffic as a change rate in the number of cars per zone, see [22] for a review on several MFD-based models. The MFD-based approach is easy in use, this makes it popular for traffic control design such as perimeter control [14], robust control [16], etc. However, only homogeneously congested areas may have a well-defined MFD. Otherwise this area must be repartitioned based on the traffic state [15], what makes MFD framework tedious in case of rapidly changing traffic conditions. Moreover, MFD approach also does not capture the particular shape of congestions, see [23].

As an alternative to MFD, one can also use two-dimensional continuum models to describe traffic in urban networks. Thus, [19] introduced an extension of the classical LWR-model to two dimensions with space-dependent FD that incorporate network infrastructure parameters. A general method to calculate steady-states in 2D-LWR was presented in [23], while [24] elaborated a boundary controller for congested traffic that was further extended to traffic being in any (mixed) regime in [25]. Another continuous 2D model presented in [13] uses the solution of the Eikonal equation to determine the direction of traffic motion.

The aforementioned references consider traffic flow that has only one direction of motion. The first attempt to include multiple directions in 2D continuum models was made only several years ago, when [18] deployed dynamic user-optimal principle for the path choice. The drawback of this model is that the traffic density may become unbounded. There exist also other works [21], [20] proposing 2D multi-layer models with bounded densities. However, these models are not necessarily hyperbolic and they do not include mixing between layers. Our recent work [26] fixes both of these aspects introducing a multi-directional model, in which the state evolves in four cardinal directions: North, South, West and East (NSWE-model). These density layers interact with each other meaning that cars might change their original direction of movement. The information about the traffic flow direction is obtained from the turning ratios at intersections.

In this paper we design a boundary control for the NSWE-model that drives an initially congested state to the best possible desired equilibrium corresponding to congestion minimization, which equivalently means throughput maximization of the network. Our main contribution is an extensive analysis of possible desired space-varying profiles that the system can achieve, which is far from being trivial for multi-directional traffic systems. Moreover, we use Lyapunov methods to show the exponential convergence to the desired state.

This work was supported by the funding from the European Research Council (ERC) under the European Union’s Horizon 2020 research and innovation programme (grant agreement 694209)

L. Tumash is with Univ. Grenoble Alpes, CNRS, Inria, Grenoble INP, GIPSA-lab, 38000 Grenoble, France, [liudmila.tumash@gipsa-lab.fr](mailto:liudmila.tumash@gipsa-lab.fr)

C. Canudas-de-Wit is with Univ. Grenoble Alpes, CNRS, Inria, Grenoble INP, GIPSA-lab, 38000 Grenoble, France, [carlos.canudas-de-wit@gipsa-lab.grenoble-inp.fr](mailto:carlos.canudas-de-wit@gipsa-lab.grenoble-inp.fr)

M. L. Delle Monache is with Univ. Grenoble Alpes, Inria, CNRS, Grenoble INP, GIPSA-Lab, 38000 Grenoble, France [ml.dellemonache@inria.fr](mailto:ml.dellemonache@inria.fr)

## II. NSWE TRAFFIC MODEL

We use the NSWE-model introduced in [26] to predict a multi-directional traffic flow evolution on a given large-scale urban network. The propagation of traffic is described in terms of vehicle density  $\rho = (\rho_N, \rho_S, \rho_W, \rho_E)^T$  defined on a bounded continuum 2D plane  $\forall(x, y) \in \Omega$  as a four-dimensional vector containing information about the density evolution in North (N), South (S), West (W) and East (E) directions. This plane  $\Omega$  is a rectangular domain bounded by  $x_{min}$ ,  $x_{max}$ ,  $y_{min}$  and  $y_{max}$  that represents an urban network, whose road parameters are interpolated everywhere in the domain as a function of the distance to these roads. Thus, the NSWE-model describes the evolution of  $\rho(x, y, t) : \Omega \times \mathbb{R}^+ \rightarrow \mathbb{R}^+$  by the following system of partial differential equations:

$$\begin{cases} \frac{\partial \rho_N}{\partial t} = \frac{1}{L} (\psi_N^{in} - \psi_N^{out}) - \frac{\partial(c_N \psi_N)}{\partial x} - \frac{\partial(s_N \psi_N)}{\partial y}, \\ \frac{\partial \rho_S}{\partial t} = \frac{1}{L} (\psi_S^{in} - \psi_S^{out}) - \frac{\partial(c_S \psi_S)}{\partial x} - \frac{\partial(s_S \psi_S)}{\partial y}, \\ \frac{\partial \rho_W}{\partial t} = \frac{1}{L} (\psi_W^{in} - \psi_W^{out}) - \frac{\partial(c_W \psi_W)}{\partial x} - \frac{\partial(s_W \psi_W)}{\partial y}, \\ \frac{\partial \rho_E}{\partial t} = \frac{1}{L} (\psi_E^{in} - \psi_E^{out}) - \frac{\partial(c_E \psi_E)}{\partial x} - \frac{\partial(s_E \psi_E)}{\partial y}. \end{cases} \quad (1)$$

The flow function  $\psi(x, y, \rho)$  is a four-dimensional vector  $\psi = (\psi_N, \psi_S, \psi_W, \psi_E)^T$ . Each of its elements is obtained from the **fundamental diagram** (FD). Let us consider the North direction to simplify the definitions. Then,  $\psi_N(x, y, \rho_N) : \Omega \times \mathbb{R}^+ \rightarrow \mathbb{R}^+$  is a concave function that achieves its unique maximum  $\psi_N^{max}(x, y) \forall(x, y) \in \Omega$  (*capacity*) at the *critical density*  $\rho_N^c(x, y)$ , and the minimum is achieved at  $\psi_N(x, y, 0) = \psi_N(x, y, \rho_N^{max}) = 0$  with  $\rho_N^{max}(x, y)$  being the space-dependent traffic jam density of the North direction. Vehicles move freely to the North with a positive kinematic wave speed  $v_N(x, y)$  if the density in this direction is below the critical value, i.e., the **free-flow regime** occurs for  $\rho_N(x, y) \in [0, \rho_N^c(x, y)] \forall(x, y) \in \Omega$ . Otherwise vehicles move in the **congested regime** with a negative kinematic wave speed  $\omega_N(x, y)$  if  $\rho_N(x, y) \in (\rho_N^c(x, y), \rho_N^{max}(x, y)] \forall(x, y) \in \Omega$ . In general, traffic flow in other directions  $\psi_S$ ,  $\psi_W$ , and  $\psi_E$  can be retrieved from FD of the corresponding directions. Fundamental diagrams can have different shapes, see [17] for a review. In this work we use the most simple fundamental diagram that has a triangular shape suggested by [7], see Fig. 1.

In (1),  $\psi^{in}(x, y, \rho) - \psi^{out}(x, y, \rho)$  is the net flow on a road:

$$\begin{pmatrix} \psi_N^{in} - \psi_N^{out} \\ \psi_S^{in} - \psi_S^{out} \\ \psi_W^{in} - \psi_W^{out} \\ \psi_E^{in} - \psi_E^{out} \end{pmatrix} = \begin{pmatrix} \psi_{SN} + \psi_{WN} + \psi_{EN} - \psi_{NS} - \psi_{NW} - \psi_{NE} \\ \psi_{NS} + \psi_{WS} + \psi_{ES} - \psi_{SN} - \psi_{SW} - \psi_{SE} \\ \psi_{NW} + \psi_{SW} + \psi_{EW} - \psi_{WN} - \psi_{WS} - \psi_{WE} \\ \psi_{NE} + \psi_{SE} + \psi_{WE} - \psi_{EN} - \psi_{ES} - \psi_{EW} \end{pmatrix}.$$

Thereby, each of the *partial flows* from one cardinal direction to another is a function of the corresponding demand and supply functions, e.g., flow of cars that were going to the South and then turned to the North  $\psi_{SN}(x, y, \rho_S, \rho_N)$  is a function of the demand from the South  $D_S$  and the supply of the North  $S_N$ :

$$\psi_{SN} = \min(\alpha_{SN} D_S(\rho_S), \beta_{SN} S_N(\rho_N)), \quad (2)$$

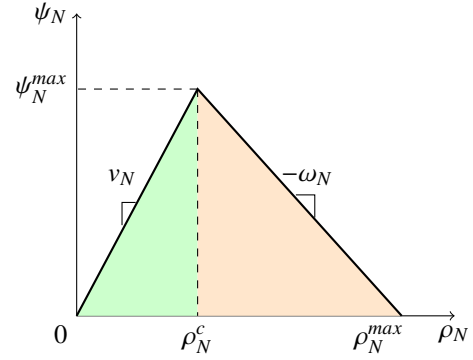


Fig. 1: Triangular FD of the North direction for some  $(x, y) \in \Omega$ : free-flow regime (area in green) and congested regime (area in orange).

where  $\alpha_{SN}$  and  $\beta_{SN}$  are the turning ratio from South to North and the supply ratio of the North for the vehicles arriving from the South, correspondingly. The demand and supply functions in (2) take the following forms:

$$D_S(\rho_S) = \begin{cases} v_S \rho_S, & \text{if } 0 \leq \rho_S \leq \rho_S^c, \\ \psi_S^{max}, & \text{if } \rho_S^c < \rho_S \leq \rho_S^{max}, \end{cases} \quad (3)$$

and

$$S_N(\rho_N) = \begin{cases} \psi_N^{max}, & \text{if } 0 \leq \rho_N \leq \rho_N^c, \\ \omega_N(\rho_N^{max} - \rho_N), & \text{if } \rho_N^c < \rho_N \leq \rho_N^{max}, \end{cases} \quad (4)$$

where the critical density  $\rho_N^c$  and the maximal flow  $\psi_N^{max}$  are defined  $\forall(x, y) \in \Omega$  as:

$$\rho_N^c = \frac{\omega_N}{v_N + \omega_N} \rho_N^{max}, \quad \psi_N^{max} = \frac{v_N \omega_N}{v_N + \omega_N} \rho_N^{max},$$

and throughout this work we also assume that  $\rho^c = \rho^{max}/3$  for all the directions.

We can now express the partial flow by inserting (4) and (3) into (2) and obtain:

$$\psi_{SN} = \min(\alpha_{SN} v_S \rho_S, \alpha_{SN} \psi_S^{max}, \beta_{SN} \omega_N (\rho_N^{max} - \rho_N), \beta_{SN} \psi_N^{max}). \quad (5)$$

If cars are moving in the free-flow regime from South to North, then (2) is resolved to the benefit of the demand function. Otherwise, if the density of the cars going from the South to the North is too high causing the congested regime, then (2) equals to the supply of the North.

In [26] the NSWE-model was originally derived to describe the density propagation in the vicinity of some intersection in a unique way. It was then extended to the network formulation when intersection parameters were defined everywhere in the continuum plane  $\Omega$  through interpolation (details are given below). Thus, if we imagine that model (1) is valid in the vicinity of some intersection located at  $(x, y)$  with  $n_{out}$  outgoing roads each having length  $l_j$  for  $j \in [1, \dots, n_{out}]$ , then  $L(x, y)$  in (1) should be interpreted as the mean length of outgoing roads of this intersection, and

it was chosen such that the number of cars is conserved:

$$L = \frac{\sum_{j=1}^{n_{out}} \rho_j^{max} l_j}{\sum_{j=1}^{n_{out}} \rho_j^{max}}$$

Finally, variables  $c_N, c_S, c_W, c_E$  and  $s_N, s_S, s_W, s_E$  from system (1) describe the general orientation of outgoing roads, e.g., consider North:

$$c_N = \frac{\sum_{j=1}^{n_{out}} p_{\theta_j}^N \cos \theta_j \psi_j^{max}}{\sum_{j=1}^{n_{out}} p_{\theta_j}^N \psi_j^{max}}, \quad s_N = \frac{\sum_{j=1}^{n_{out}} p_{\theta_j}^N \sin \theta_j \psi_j^{max}}{\sum_{j=1}^{n_{out}} p_{\theta_j}^N \psi_j^{max}},$$

where  $p_{\theta_j}^N \in [0, 1]$  is a coefficient indicating the orientation of road  $j$  with respect to the North direction (1 means that road  $j$  is pointing exactly to the North, 0 means that the angle is larger than  $\pi/2$  with the North direction).

It was shown in [26] that the flow in any direction, e.g.  $\psi_N$ , can be simplified to the minimum between the demand  $D_N$  and supply  $S_N$  functions of this direction, i.e.,

$$\psi_N = \min(D_N(\rho_N), S_N(\rho_N)), \quad (6)$$

if we assume that the network is well-designed in terms of maximal flows, e.g. consider flow from South to West:

$$\alpha_{SN} \psi_N^{max} = \beta_{SN} \psi_S^{max}.$$

This assumption means that vehicles moving to the South at maximum capacity continue moving at maximum capacity after they turn to the North at an intersection.

The urban network, on which we model traffic propagation, is always given as a set of physical roads and intersections with given speed limits and the number of lanes. However, the NSWE-model (1) being continuous requires that all the intersection and FD parameters are defined  $\forall(x, y) \in \Omega$ . We achieve that by applying interpolation methods. First, we define the maximal density  $\rho^{max}$  by placing every  $6m$  a vehicle on every road. We assume that each such vehicle contributes to the global density with a Gaussian kernel with standard deviation  $50m$  centred at its position  $\forall(x, y) \in \Omega$  (see [19]). Further, we project all the intersection and FD parameters  $\alpha, \beta, L, \cos \theta, \sin \theta, \rho^{max}$  and the parameters of fundamental diagram  $v$  and  $\omega$  into NSWE-formulation using network's geometric properties. In [26] it is extensively described how to project the intersection and FD parameters into NSWE-formulation using projection coefficients  $p^N, p^S, p^W, p^E$ . Then, we interpolate all these variables using Inverse Distance Weighting, e.g., for the average road length we get

$$L(x, y) = \frac{\sum_{k=1}^N L(x_k, y_k) e^{-\eta \sqrt{(x-x_k)^2 + (y-y_k)^2}}}{\sum_{k=1}^N e^{-\eta \sqrt{(x-x_k)^2 + (y-y_k)^2}}}, \quad \forall(x, y) \in \Omega \quad (7)$$

where  $N$  is the number of intersections in the network, and  $\eta$  is the interpolation parameter used to denote the sensitivity to the distance from the real roads. If we want to follow the global trend of the flow motion, we choose  $\eta$  to be small, otherwise we choose larger values of  $\eta$  in order to follow the underlying network topology, see [19].

### III. PROBLEM STATEMENT

In the following we will state the control problem of driving congested traffic to some desired space-varying profile. This desired state corresponds to congestion minimization under the constraint that supply values at the boundaries are proportional to the maximal density (details are given below).

#### A. Congested Traffic

In a congested system the minimum in equation (6) is always resolved to the benefit of supply, and traffic operates at or above its critical density, which in turn implies for (5) that

$$\psi_{SN} = \beta_{SN} \omega_N (\rho_N^{max} - \rho_N), \quad \forall(x, y) \in \Omega.$$

Using this expression and fixing  $\rho_0(x, y) \forall(x, y) \in \Omega$  as an initial condition, we can now introduce the following Initial Boundary Value Problem from the NSWE-model (1) that describes the congested traffic flow dynamics on a compact domain  $\Omega$  with  $\Gamma \in \Omega$  being its boundary:

$$\begin{cases} \frac{\partial \rho}{\partial t} = \frac{1}{L} (I - B) W (\rho^{max} - \rho) - \frac{\partial [C W (\rho^{max} - \rho)]}{\partial x} \\ \quad - \frac{\partial [S W (\rho^{max} - \rho)]}{\partial y}, \quad (8) \\ \rho(x, y, t) = u(x, y, t), \quad \forall(x, y) \in \Gamma_{out} \\ \rho(x, y, 0) = \rho_0(x, y), \end{cases}$$

where  $\Gamma_{out} \subset \Gamma$  is a set of boundary points  $(x, y)$  associated with the domain's exit:

$$\Gamma_{out} = (y_{max}, y_{min}, x_{min}, x_{max})^T.$$

The state of (8) is controlled at the upstream boundary  $\Gamma_{out}$  by specifying the control vector  $u = (u_N, u_S, u_W, u_E)^T$ .

Finally,  $C, S, W$  and  $B$  in (8) are all  $4 \times 4$  matrices such that  $C$  and  $S$  are diagonal matrices,  $W$  is a positive-definite diagonal matrix, and  $B$  is a nonnegative matrix:

$$C = \begin{bmatrix} c_N & 0 & 0 & 0 \\ 0 & c_S & 0 & 0 \\ 0 & 0 & c_W & 0 \\ 0 & 0 & 0 & c_E \end{bmatrix}, \quad S = \begin{bmatrix} s_N & 0 & 0 & 0 \\ 0 & s_S & 0 & 0 \\ 0 & 0 & s_W & 0 \\ 0 & 0 & 0 & s_E \end{bmatrix},$$

$$W = \begin{bmatrix} \omega_N & 0 & 0 & 0 \\ 0 & \omega_S & 0 & 0 \\ 0 & 0 & \omega_W & 0 \\ 0 & 0 & 0 & \omega_E \end{bmatrix}, \quad B = \begin{bmatrix} \beta_{NN} & \beta_{NS} & \beta_{NW} & \beta_{NE} \\ \beta_{SN} & \beta_{SS} & \beta_{SW} & \beta_{SE} \\ \beta_{WN} & \beta_{WS} & \beta_{WW} & \beta_{WE} \\ \beta_{EN} & \beta_{ES} & \beta_{EW} & \beta_{EE} \end{bmatrix}.$$

#### B. Desired Equilibrium

Let us define the error of the state from the desired space-varying equilibrium  $\rho_d(x, y) \forall(x, y) \in \Omega$  as:

$$\tilde{\rho}(x, y, t) = \rho(x, y, t) - \rho_d(x, y).$$

To simplify the mathematical analysis, we restrict our study to desired profiles having values only in the congested regime, i.e.,  $\rho_d(x, y) > \rho_c(x, y) \forall(x, y) \in \Omega$ .

The time derivatives of state and error coincide, which in combination with (8) results into

$$\frac{\partial \tilde{\rho}}{\partial t} = \frac{1}{L}(I-B)W(\rho^{max} - \rho_d - \tilde{\rho}) - \frac{\partial[CW(\rho^{max} - \rho_d - \tilde{\rho})]}{\partial x} - \frac{\partial[S W(\rho^{max} - \rho_d - \tilde{\rho})]}{\partial y}. \quad (9)$$

Let us now write the dynamics for the desired density:

$$\frac{\partial \rho_d}{\partial t} = 0 = \frac{1}{L}(I-B)W(\rho^{max} - \rho_d) - \frac{\partial[CW(\rho^{max} - \rho_d)]}{\partial x} - \frac{\partial[S W(\rho^{max} - \rho_d)]}{\partial y}. \quad (10)$$

If we subtract (10) from (9), we also obtain the error term dynamics:

$$\frac{\partial \tilde{\rho}}{\partial t} = \frac{1}{L}(B-I)W\tilde{\rho} + \frac{\partial[CW\tilde{\rho}]}{\partial x} + \frac{\partial[S W\tilde{\rho}]}{\partial y}. \quad (11)$$

In this work our goal is to find a desired density distribution that corresponds to congestion minimization, and then to design a boundary control that stabilizes the density to that desired equilibrium. Thereby, the desired density profile must remain in the congested regime, i.e.  $\rho_d(x,y) > \rho^c(x,y) \forall (x,y) \in \Omega$ , and its values at the boundaries should be proportional to the maximal densities at the corresponding boundary coordinates, i.e.,  $\exists \gamma \in [1/3, 1]$  such that

$$\rho_d(x,y) = \gamma \rho^{max}(x,y), \quad \forall (x,y) \in \Gamma_{out}. \quad (12)$$

The range of constant  $\gamma$  is related to the requirement for  $\rho_d$  to stay in the congested regime, since with  $\gamma = 1/3$  the desired state equals the critical density  $\rho_c$  (recall that we have chosen  $\rho_c = 1/3\rho^{max}$ ). Thus, we need to determine constant  $\gamma$  that provides congestion minimization given (12).

**Problem 1.** Find the desired space-dependent density  $\rho_d(x,y) \forall (x,y) \in \Omega$  that minimizes congestion under the constraints that  $\rho_d(x,y) \geq \rho^c(x,y) \forall (x,y) \in \Omega$  and that boundary values are proportional to the maximal densities (12).

**Remark 1.** Minimizing congestion means finding  $\rho_d(x,y) \geq \rho^c(x,y) \forall (x,y) \in \Omega$  for which  $\min(\rho_d - \rho^c)$  is achieved.

**Remark 2.** Physically, a proportional relation of the density values at the boundaries to the corresponding maximal densities (12) implies that boundaries are filled in a homogeneous way, i.e., supply at the boundaries is nearly the same. This might be useful in a situation when vehicles concentrated in a city center want to leave it simultaneously, e.g., when vehicles return back home from their offices.

In order to find a desired profile satisfying Problem 1, we need to solve a PDE (10) that describes its structural dependence on  $(x,y)$ . For this we need to introduce a change of variables  $\hat{\rho}(x,y) \forall (x,y) \in \Omega$  as

$$\hat{\rho}(x,y) = \rho^{max}(x,y) - \rho_d(x,y), \quad (13)$$

which being inserted into (10), yields

$$\frac{1}{L}(I-B)W\hat{\rho} = \frac{\partial[CW\hat{\rho}]}{\partial x} + \frac{\partial[S W\hat{\rho}]}{\partial y}. \quad (14)$$

We compute the desired state  $\rho_d \forall (x,y) \in \Omega$  by performing the following steps:

1) *Step 1:* Set the desired density values at the upstream boundaries  $\Gamma_{out}$  equal to the corresponding critical values, i.e., pick up the lowest  $\gamma = 1/3$ , which leads to

$$\hat{\rho}(x,y) = \frac{2}{3}\rho^{max}(x,y), \quad \forall (x,y) \in \Gamma_{out}.$$

2) *Step 2:* Discretize the plane corresponding to Grenoble network  $(x,y) \in \Omega$  of the size  $M = 1.4km$  (as in Fig. 2) into 3600 equal cells ( $N_x = 60$  in  $x$  dimension and  $N_y = 60$  in  $y$  dimension). Thereby, each cell is now described by an index pair  $(i,j)$ , where  $i = [1, \dots, N_x]$  and  $j = [1, \dots, N_y]$ . The discretization steps  $\Delta x$  and  $\Delta y$  can be found as

$$\Delta x = \frac{M}{N_x} \quad \text{and} \quad \Delta y = \frac{M}{N_y}.$$

3) *Step 3:* Discretize the PDE system given by (14). For convenience we consider the North direction, and then the same steps should be done for the remaining directions. In accordance with the upwind scheme [1] used to provide the correct direction of information propagation in a flow field, the discretization scheme of  $c_N \omega_N \hat{\rho}_N$  and  $s_N \omega_N \hat{\rho}_N$  depends on the signs of  $c_N$  and  $s_N$ , i.e.  $\forall (i,j) \in [1, \dots, N_x] \times [1, \dots, N_y]$ :

$$c_{N,i,j} > 0 : \frac{c_{N,i+1,j} \omega_{N,i+1,j} \hat{\rho}_{N,i+1,j} - c_{N,i,j} \omega_{N,i,j} \hat{\rho}_{N,i,j}}{\Delta x},$$

$$c_{N,i,j} < 0 : \frac{c_{N,i,j} \omega_{N,i,j} \hat{\rho}_{N,i,j} - c_{N,i-1,j} \omega_{N,i-1,j} \hat{\rho}_{N,i-1,j}}{\Delta x}.$$

The same can be written for  $s_N$  and for  $y$ -direction, for which we fix  $i$  and vary  $j$ .

We also define  $4 \times 4$  diagonal matrices  $Q_x$ ,  $Q_y$ ,  $R_x$  and  $R_y$  as

$$c_{N,i,j} > 0 : Q_{xNN,i,j} = \frac{c_{N,i+1,j} \omega_{N,i+1,j}}{\Delta x}, \quad R_{xNN,i,j} = 0,$$

else :

$$Q_{xNN,i,j} = 0, \quad R_{xNN,i,j} = -\frac{c_{N,i-1,j} \omega_{N,i-1,j}}{\Delta x},$$

and the same can be written for  $s_N$  and  $y$ -direction with varying  $j$  and fixed  $i$ .

4) *Step 4:* Define also a  $4 \times 4$  matrix  $P$  as:

$$P_{i,j} = \frac{1}{L_{i,j}}(B_{i,j} - \mathbb{I})W_{ij} - \frac{|C_{i,j}|W_{i,j}}{\Delta x} - \frac{|S_{i,j}|W_{i,j}}{\Delta y}.$$

Using the definition of matrices  $P$ ,  $Q_x$ ,  $Q_y$ ,  $R_x$  and  $R_y$ , we can now write the PDE system for  $\hat{\rho}$  given by (14) in a discretized form that reads  $\forall (i,j) \in [1, \dots, N_x] \times [1, \dots, N_y]$ :

$$P_{i,j} \hat{\rho}_{i,j} + Q_{x,i,j} \hat{\rho}_{i+1,j} + Q_{y,i,j} \hat{\rho}_{i,j+1} + R_{x,i,j} \hat{\rho}_{i-1,j} + R_{y,i,j} \hat{\rho}_{i,j-1} = 0. \quad (15)$$

Notice that  $\hat{\rho}_{0,j}$ ,  $\hat{\rho}_{N_x+1,j}$ ,  $\hat{\rho}_{i,0}$ ,  $\hat{\rho}_{i,N_y+1}$  take the values from the boundary conditions.

5) *Step 5:* System (15) is solved using the Alternating Direction Implicit method (dimensional splitting, see [2]). At each iteration first  $x$  and then  $y$  steps are performed. At each  $x$  step the terms  $\hat{\rho}_{i,j-1}$  and  $\hat{\rho}_{i,j+1}$  take fixed values from the previous iteration, while  $\hat{\rho}_{i-1,j}$  and  $\hat{\rho}_{i+1,j}$  are fixed for each  $y$  step. At  $x$  step our system (15) is solved for every  $j$  by the block tridiagonal matrix algorithm, while at  $y$  step this algorithm is applied for every column  $i$ .

6) *Step 6:* Since system (15) is linear,  $\alpha\hat{\rho}$  is also a solution to this system for some  $\alpha \in [0, 1]$ . Let us now come back to the desired state  $\rho_d$  that we can get from (13):

$$\rho_d = \rho^{max} - \alpha\hat{\rho}.$$

By choosing  $\alpha = 0$  we obtain  $\rho_d = \rho^{max}$ , while by choosing  $\alpha = 1$  we achieve  $\rho_d = \rho^c$  at the boundaries, (see step 1 and use  $\rho^c = 1/3\rho^{max}$ ). This implies that by taking an intermediate value of  $\alpha$  we guarantee the congested regime at the boundaries. Let us calculate  $\alpha^*$  that provides for the desired state  $\rho_d$  to be as close as possible to  $\rho^c$  while staying in the congested regime, for which in general we can write:

$$\begin{aligned} \frac{\rho_d}{\rho^c} \geq 1 &\Rightarrow \frac{\rho^{max} - \alpha\hat{\rho}}{1/3\rho^{max}} \geq 1 \Rightarrow 3 - 3\alpha\frac{\hat{\rho}}{\rho^{max}} \geq 1 \\ &\Rightarrow \alpha \leq \frac{2}{3}\frac{\rho^{max}}{\hat{\rho}}, \quad \forall(x,y) \in \Omega. \end{aligned}$$

It follows from the discussion above that the optimal state is achieved if  $\exists(x^*, y^*)$ , for which

$$\alpha^* = \min_{\substack{(x,y) \in \Omega \\ r \in \{N,S,W,E\}}} \frac{2\rho_r^{max}(x,y)}{3\hat{\rho}_r(x,y)}. \quad (16)$$

To get an expression for the desired profile at the boundaries  $\rho_d(x,y) \forall(x,y) \in \Gamma_{out}$ , we express  $\rho_d$  from (13) and set it equal to (12), which yields

$$\rho^{max} - \alpha\hat{\rho} = \gamma\rho^{max}. \quad (17)$$

We take the boundary value of  $\hat{\rho}$  from step 1, insert it into (17), and we finally obtain

$$\rho_d = \left(1 - \frac{2}{3}\alpha^*\right)\rho^{max} \Rightarrow \gamma^* = 1 - \frac{2}{3}\alpha^*. \quad (18)$$

#### IV. BOUNDARY CONTROL DESIGN

The aim of this section is to design a boundary control such that the density achieves the desired profile obtained in the previous section (18). This is formalized as follows.

**Problem 2.** Find a boundary controller such that a congested density from system (8) converges to the desired space-varying density  $\rho_d(x,y)$  given by (18)  $\forall(x,y) \in \Omega$  as  $t \rightarrow \infty$ .

In order to prove the convergence to the desired profile, we have to assume that the main direction of the density transportation coincides with the cardinal direction, which for example holds for a Manhattan grid type of traffic networks.

**Assumption 1.** The matrices  $C$  and  $S$  from (8) are constant in space, e.g., they can be defined as:

$$\begin{aligned} c_N = 0, \quad c_S = 0, \quad c_W = -1, \quad c_E = 1, \\ s_N = 1, \quad s_S = -1, \quad s_W = 0, \quad s_E = 0. \end{aligned} \quad (19)$$

In general, the further analysis requires these variables to be just constant in space, but we choose (19) for simplicity. We also make an assumption on supply coefficients:

**Assumption 2.** Supply coefficient matrix  $B$  is constant in space, which in turn implies that every intersection has the same turning ratio pattern.

**Theorem 1.** Under Assumptions 1 and 2, let the boundary controller be defined as

$$u(x,y) = \begin{pmatrix} \rho_{d,N}(x,y_{max}) \\ \rho_{d,S}(x,y_{min}) \\ \rho_{d,W}(x_{min},y) \\ \rho_{d,E}(x_{max},y) \end{pmatrix}, \quad \forall(x,y) \in \Gamma_{out}, \quad (20)$$

then  $\exists K, k > 0$  such that

$$\|\rho(t) - \rho_d\|_{L^2}^2 \leq e^{-kt} K \|\rho(0) - \rho_d\|_{L^2}^2,$$

i.e., the state  $\rho(x,y,t)$  exponentially converges to the desired equilibrium  $\rho_d(x,y) \forall(x,y) \in \Omega$  as  $t \rightarrow \infty$ .

**Remark 3.** Although for the simplicity of the proof we assumed a regular Manhattan grid structure (Assumptions 1 and 2), control (20) can be applied to a more general network, as we will show on a numerical example for which we take the network of Grenoble downtown.

*Proof of Theorem 1.* Let us first analyse matrix  $B - I$ . Its non-diagonal elements are positive and its diagonal elements are negative. Moreover,  $B - I$  has one eigenvalue equal to zero and all others are negative, see Appendix I. Therefore,  $B - I$  is a negative singular M-matrix with one zero eigenvalue. Thus, there exists a positive-definite diagonal  $4 \times 4$  matrix  $D$  such that

$$D(B - I) + (B^T - I)D \leq 0. \quad (21)$$

Let us also introduce a diagonal  $4 \times 4$  matrix composed by exponential functions as follows:

$$E = \begin{bmatrix} e^y & 0 & 0 & 0 \\ 0 & e^{-y} & 0 & 0 \\ 0 & 0 & e^{-x} & 0 \\ 0 & 0 & 0 & e^x \end{bmatrix}.$$

We define the following Lyapunov function candidate:

$$\begin{aligned} V = \int_{x_{min}}^{x_{max}} \int_{y_{min}}^{y_{max}} \tilde{\rho}^T WDE\tilde{\rho} dy dx = \int_{x_{min}}^{x_{max}} \int_{y_{min}}^{y_{max}} (\tilde{\rho}_N^2 \omega_N D_N e^y \\ + \tilde{\rho}_S^2 \omega_S D_S e^{-y} + \tilde{\rho}_W^2 \omega_W D_W e^{-x} + \tilde{\rho}_E^2 \omega_E D_E e^x) dy dx, \end{aligned} \quad (22)$$

where  $D_N \dots D_E$  are the diagonal elements of matrix  $D$ .

The function (22) is obviously positive-definite, since matrix  $WDE > 0$ . Let us now take its time derivative, which yields

$$\dot{V} = \int_{x_{min}}^{x_{max}} \int_{y_{min}}^{y_{max}} 2 \frac{\partial \tilde{\rho}^T}{\partial t} WDE\tilde{\rho} dy dx, \quad (23)$$

where the error dynamics  $\partial\tilde{\rho}/\partial t$  should be taken from (11), which allows us to further expand (23) as:

$$\begin{aligned} \dot{V} &= \int_{x_{\min}}^{x_{\max}} \int_{y_{\min}}^{y_{\max}} \frac{1}{L} (W\tilde{\rho})^T \left( DE(B-I) + (B^T - I)DE \right) W\tilde{\rho} dy dx \\ &+ 2 \int_{x_{\min}}^{x_{\max}} \int_{y_{\min}}^{y_{\max}} (W\tilde{\rho})^T DE \left( \frac{\partial[CW\tilde{\rho}]}{\partial x} + \frac{\partial[S W\tilde{\rho}]}{\partial y} \right) dy dx. \end{aligned} \quad (24)$$

Let us now denote the first term of (24) as  $\dot{V}_1$  and the second terms as  $\dot{V}_2$ . The term  $\dot{V}_1$  is negative due to (21) and the fact that matrix  $E$  is non-negative, i.e.,

$$\dot{V}_1 = \int_{x_{\min}}^{x_{\max}} \int_{y_{\min}}^{y_{\max}} \frac{1}{L} (W\tilde{\rho})^T \left( DE(B-I) + (B^T - I)DE \right) W\tilde{\rho} dy dx < 0.$$

We further consider  $\dot{V}_2$  by inserting the values of matrices  $C$  and  $S$  from assumption (19):

$$\begin{aligned} \dot{V}_2 &= 2 \int_{x_{\min}}^{x_{\max}} \int_{y_{\min}}^{y_{\max}} \left( \omega_E \tilde{\rho}_E DE e^x \frac{\partial(\omega_E \tilde{\rho}_E)}{\partial x} - \omega_W \tilde{\rho}_W DW e^{-x} \frac{\partial(\omega_W \tilde{\rho}_W)}{\partial x} \right. \\ &\quad \left. + \omega_N \tilde{\rho}_N DN e^y \frac{\partial(\omega_N \tilde{\rho}_N)}{\partial y} - \omega_S \tilde{\rho}_S DS e^{-y} \frac{\partial(\omega_S \tilde{\rho}_S)}{\partial y} \right) dy dx. \end{aligned}$$

This expression is then integrated by parts, which yields:

$$\begin{aligned} \dot{V}_2 &= \int_{y_{\min}}^{y_{\max}} \left[ e^{-x} (\sqrt{D_W} \omega_W \tilde{\rho}_W)^2 - e^x (\sqrt{D_E} \omega_E \tilde{\rho}_E)^2 \right]_{x=x_{\min}}^{x_{\max}} dy \\ &+ \int_{y_{\min}}^{y_{\max}} \left[ e^x (\sqrt{D_E} \omega_E \tilde{\rho}_E)^2 - e^{-x} (\sqrt{D_W} \omega_W \tilde{\rho}_W)^2 \right]_{x=x_{\max}}^{x_{\min}} dy \\ &+ \int_{x_{\min}}^{x_{\max}} \left[ e^{-y} (\sqrt{D_S} \omega_S \tilde{\rho}_S)^2 - e^y (\sqrt{D_N} \omega_N \tilde{\rho}_N)^2 \right]_{y=y_{\min}}^{y_{\max}} dx \\ &+ \int_{x_{\min}}^{x_{\max}} \left[ e^y (\sqrt{D_N} \omega_N \tilde{\rho}_N)^2 - e^{-y} (\sqrt{D_S} \omega_S \tilde{\rho}_S)^2 \right]_{y=y_{\max}}^{y_{\min}} dx \\ &- \int_{x_{\min}}^{x_{\max}} \int_{y_{\min}}^{y_{\max}} \left( e^x DE (\omega_E \tilde{\rho}_E)^2 + e^{-x} DW (\omega_W \tilde{\rho}_W)^2 \right. \\ &\quad \left. + e^y DN (\omega_N \tilde{\rho}_N)^2 + e^{-y} DS (\omega_S \tilde{\rho}_S)^2 \right) dy dx. \end{aligned} \quad (25)$$

By setting  $\forall t \in \mathbb{R}^+$

$$\begin{aligned} \tilde{\rho}_N(x, y_{\max}, t) &= 0, \quad \tilde{\rho}_S(x, y_{\min}, t) = 0, \quad \forall x \in [x_{\min}, x_{\max}], \\ \tilde{\rho}_W(x_{\min}, y, t) &= 0, \quad \tilde{\rho}_E(x_{\max}, y, t) = 0, \quad \forall y \in [y_{\min}, y_{\max}], \end{aligned} \quad (26)$$

one ensures that the first four integrals in (25) go to zero.

The last term in (25) can be bounded as follows

$$\begin{aligned} &\int_{x_{\min}}^{x_{\max}} \int_{y_{\min}}^{y_{\max}} \left( e^x DE (\omega_E \tilde{\rho}_E)^2 + e^{-x} DW (\omega_W \tilde{\rho}_W)^2 \right. \\ &\quad \left. + e^y DN (\omega_N \tilde{\rho}_N)^2 + e^{-y} DS (\omega_S \tilde{\rho}_S)^2 \right) dy dx \\ &\leq - \min_{\substack{(x,y) \in \Omega \\ r \in \{N,S,W,E\}}} \omega_r(x,y) \int_{x_{\min}}^{x_{\max}} \int_{y_{\min}}^{y_{\max}} \left( e^x DE \omega_E \tilde{\rho}_E^2 \right. \\ &\quad \left. + e^{-x} DW \omega_W \tilde{\rho}_W^2 + e^y DN \omega_N \tilde{\rho}_N^2 + e^{-y} DS \omega_S \tilde{\rho}_S^2 \right) dy dx, \end{aligned} \quad (27)$$

where we have used the fact that the kinematic wave speed is positive by definition, i.e.,  $\omega > 0$ .

The integral on the right hand side of (27) coincides with the Lyapunov function (22). This means that by inserting (26) into (25) and also by using the bound from (27), we can write:

$$\dot{V} = \dot{V}_1 + \dot{V}_2 \leq \dot{V}_2 \leq -kV,$$

where  $k \in \mathbb{R}^+$  is a positive constant

$$k = \min_{\substack{(x,y) \in \Omega \\ r \in \{N,S,W,E\}}} \omega_r(x,y).$$

One can also prove that the state  $\tilde{\rho}$  converges to zero in  $L_2$  norm exponentially. Indeed, note that  $V$  defines an equivalent norm on the density space:

$$m \|\tilde{\rho}\|_{L^2}^2 \leq V \leq M \|\tilde{\rho}\|_{L^2}^2$$

with

$$m = \min_{\substack{(x,y) \in \Omega \\ r \in \{N,S,W,E\}}} \omega_r(x,y) D_r E_r(x,y),$$

$$M = \max_{\substack{(x,y) \in \Omega \\ r \in \{N,S,W,E\}}} \omega_r(x,y) D_r E_r(x,y).$$

By exponential convergence of Lyapunov functions we have

$$V(t) \leq e^{-kt} V(0),$$

therefore

$$\|\tilde{\rho}(t)\|_{L^2}^2 \leq e^{-kt} \frac{M}{m} \|\tilde{\rho}(0)\|_{L^2}^2.$$

□

**Remark 4.** Assumption 2 on space-independent  $B$  can be relaxed, if it is possible to find such a matrix  $D$  that satisfies inequality (21) and whose elements  $D_E(y)$  and  $D_W(y)$  may depend on  $y$ , while  $D_N(x)$  and  $D_S(x)$  may depend on  $x$ .

## V. NUMERICAL EXAMPLE

Finally, we demonstrate how a boundary control given by (20) works in practice using Grenoble downtown with a total surface of around  $1.4 \text{ km}^2$  as a network. We use the classical Godunov scheme [5] for the numerical simulation of system (8) under control (20) with a fully congested initial state

$$\rho_0(x,y) = \rho_{\max}(x,y), \quad \forall (x,y) \in \Omega.$$

As interpolation parameter in (7) we take  $\eta = 5$ , which is a relatively low value implying that we want to follow the global trend of motion. On Fig. 2a) we depict the

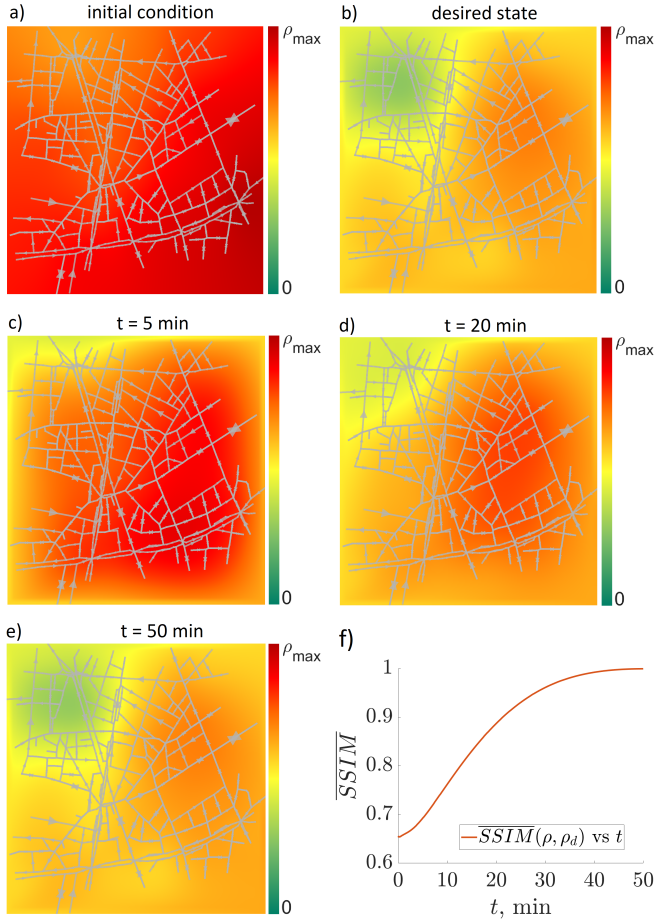


Fig. 2: Boundary control in Grenoble downtown: a) initial congested state  $\rho_0$ , b) desired equilibrium  $\rho_d$ ; controlled state at: c)  $t = 5mn$ , d)  $t = 20mn$ , e)  $t = 50mn$ ; d)  $\overline{SSIM}$  between the state and the desired density as a function of time.

fully congested state (initial condition) to be controlled, and on Fig. 2b) we depict the desired profile  $\rho_d$  obtained by following all the steps in Section III. Recall that the desired state corresponds to the congestion minimization (see Problem 1), and the coefficient  $\alpha^*$  from (17) is  $\alpha^* = 0.51$ . Further, we show the impact of boundary control on our state after  $t = 5min$  on Fig. 2c),  $t = 20min$  on Fig. 2d) and  $t = 50min$  on Fig. 2e). We can see that the state at  $t = 50min$  visually resembles the desired state from Fig. 2b).

We deploy the Structural Similarity Index (SSIM) [8] to enable a quantitative comparison between the controlled state on Fig. 2c) - e) and the desired state on Fig. 2b). Thus, the SSIM index between density distributions  $\rho$  and  $\rho_d$  can be computed as

$$SSIM(\rho, \rho_d) = \frac{(2\mu_1\mu_2 + c)(2\sigma_{12} + c)}{(\mu_1^2 + \mu_2^2 + c)(\sigma_1^2 + \sigma_2^2 + c)}, \quad (28)$$

where  $\mu_1$  and  $\mu_2$  are the mean values,  $\sigma_1$  and  $\sigma_2$  are the standard deviations, while  $\sigma_{12}$  is the correlation coefficient between the density distributions  $\rho$  and  $\rho_d$ . Finally,  $c > 0$  in (28) is a small constant that is added to avoid that the

denominator becomes zero (here we take  $c = 1 \cdot 10^{-13}$ ).

This index is a perception-based metric used to detect structural changes. The range of SSIM is  $[-1, 1]$ , where  $SSIM = 1$  means that two images are identical and  $SSIM = -1$  indicates that the second image is inverse of the first. To refine the computations, we also divide the network of Grenoble into 9 equal zones, i.e.,  $N_{zones} = 9$ . The SSIM index is then calculated for every zone of the domain, and then its mean value  $\overline{SSIM}$  is computed as:

$$\overline{SSIM}(\rho, \rho_d) = \frac{1}{N_{zones}} \sum_{l=1}^{N_{zones}} SSIM(l). \quad (29)$$

The result is shown on Fig. 2f), where the SSIM index converges to 1 indicating that the state converges to the desired profile.

## VI. CONCLUSIONS

We investigated the multi-directional NSWE model from the control perspective. In particular, we analysed the class of desired equilibria that must satisfy a certain system of PDEs. We have posed and solved the problem of finding an equilibrium state that provides congestion minimization in a network, under the constraint that its range must remain in the congested regime. The desired state was assumed to be proportional to the maximal densities at the boundaries. Further, we proved the exponential convergence of a congested state to this desired equilibrium using Lyapunov methods. Finally, we used the real network of Grenoble downtown to produce a numerical example that stays in a good agreement with the theoretical result. Thereby, at each time step we have calculated the structural similarity index to show the convergence of our density distribution to the desired one.

An appealing direction for future studies might be finding equilibria that admit mixed traffic regimes. Another possible extension may include elaborating boundary control with the constraint that the activation boundary is a set of points on real roads rather than a continuous line.

## APPENDIX I

### EIGENVALUES OF MATRIX $B - I$

Let us now analyse eigenvalues of matrix  $B - I$  from (8). To simplify the notations, we introduce  $\bar{B} = B - I$ :

$$\bar{B} = \begin{pmatrix} \beta_{NN} - 1 & \beta_{NS} & \beta_{NW} & \beta_{NE} \\ \beta_{SN} & \beta_{SS} - 1 & \beta_{SW} & \beta_{SE} \\ \beta_{WN} & \beta_{WS} & \beta_{WW} - 1 & \beta_{WE} \\ \beta_{EN} & \beta_{ES} & \beta_{EW} & \beta_{EE} - 1 \end{pmatrix} \quad (30)$$

By Gershgorin circle theorem, every eigenvalue of  $\bar{B}$  lies within at least one of the Gershgorin discs  $d(\bar{b}_{ii}, R_i)$ , where  $d$  is a closed disc centered at  $\bar{b}_{ii}$  with radius  $R_i = \sum_{j \neq i} |\bar{b}_{ji}|$ .

Consider the first row of matrix  $\bar{B}$  given by (30). The Gershgorin disc is centred at  $\beta_{NN} - 1$  and its radius is  $R_1 = \beta_{NS} + \beta_{NW} + \beta_{NE} = 1 - \beta_{NN}$ . The remaining rows of matrix  $\bar{B}$  can be analysed in exactly the same way. Due to the Gershgorin theorem, in general, every result looks similar to:

$$|\lambda - (\beta_{NN} - 1)| \leq (1 - \beta_{NN}),$$

which implies that  $\operatorname{Re}\lambda(\bar{B}) \leq 0 \forall \lambda(\bar{B})$  and if  $\operatorname{Re}\lambda(\bar{B}) = 0$ , then  $\lambda(\bar{B}) = 0$ .

Let us consider  $\lambda(\bar{B}) = 0$  with  $x$  being the corresponding eigenvector:

$$x^T \bar{B} = 0 = x^T \lambda(\bar{B}).$$

Using the definition of matrix  $\bar{B}$ , we further get

$$x^T (B - \mathbb{I}) = 0 \Rightarrow x^T B = x^T.$$

Thus, it follows that  $x$  is also the eigenvector of matrix  $B$  associated with the eigenvalue  $\lambda(B) = 1$ .

Note that matrix  $B$  is a positive matrix, i.e.,  $\beta_{ij} > 0$  for  $1 \leq i, j \leq 4$  (assume we have no zero turning ratios). Then by Perron-Frobenius theorem  $\lambda(B) = 1$  is a Perron root (since all columns of  $B$  sum to 1), and thus it is a simple root. It follows that all the eigenvalues of matrix  $\bar{B} = (B - \mathbb{I})$  are strictly negative and only one eigenvalue is zero.

#### ACKNOWLEDGEMENT

The Scale-FreeBack project has received funding from the European Research Council (ERC) under the European Union's Horizon 2020 research and innovation programme (grant agreement N 694209).

#### REFERENCES

- [1] R. Courant, E. Isaacson and M. Rees, "On the Solution of Nonlinear Hyperbolic Differential Equations by Finite Differences", *Communications on Pure and Applied Math.*, vol. 5, pp. 243-255, 1952.
- Peaceman, D. W.; Rachford Jr., H. H. (1955), "The numerical solution of parabolic and elliptic differential equations", *Journal of the Society for Industrial and Applied Mathematics*, 3 (1): 28–41, doi:10.1137/0103003, hdl:10338.dmlcz/135399, MR 0071874.
- [2] D. W. Peaceman and H. H. Rachford Jr., "The numerical solution of parabolic and elliptic differential equations", *Journal of the Society for Industrial and Applied Mathematics*, vol. 3, no. 1, pp. 28-41, 1955.
- [3] M. Lighthill and G. Whitham, "On kinematic waves, II: A theory of traffic flow on long crowded roads", *Proc. Royal Soc. London*, vol. 229, no. 1178, pp. 317-345, 1956.
- [4] P. Richards, "Shock waves on the highway", *Operations Res.*, vol. 47, no. 1, pp. 42-51, 1956.
- [5] S. K. Godunov, "A difference method for numerical calculation of discontinuous solutions of the equations of hydrodynamics", *Matematicheskii Sbornik*, vol. 47, no. 3, pp. 271-306, 1959.
- [6] J. C. Williams, H. S. Mahmassani and R. Herman, "Urban traffic network flow models", *Transportation Research Record*, vol. 1112, pp. 78-88, 1987.
- [7] C. F. Daganzo, "The cell transmission model: A dynamic representation of highway traffic consistent with the hydrodynamic theory", *Transp. Res. Part B: Method.*, vol. 28, no. 4, pp. 269-287, 1994.
- [8] Z. Wang, A. C. Bovik, H. R. Sheikh and E. P. Simoncelli, "Image quality assessment: from error visibility to structural similarity", *IEEE Transactions on Image Processing*, vol. 13, no. 4, pp. 600-612, 2004.
- [9] A. K. Ziliaskopoulos, S. T. Waller, Y. Li and M. Byram, "Large-scale dynamic traffic assignment: implementation issues and computational analysis", *Journal of Transportation Engineering*, vol. 130, no. 5, pp. 585-593, 2004.
- [10] J. P. Lebaque, "First-order macroscopic traffic flow models: Intersection modeling, network modeling", *16th International Symposium on Transportation and Traffic Theory*, 2005.
- [11] C. F. Daganzo and N. Geroliminis, "An analytical approximation for the macroscopic fundamental diagram of urban traffic", *Trans. Res. Part B: Method.*, vol. 42, no. 9, pp. 771-781, 2008.
- [12] N. Geroliminis and C. F. Daganzo, "Existence of urban-scale macroscopic fundamental diagrams: Some experimental findings", *Trans. Res. Part B: Methodological*, vol. 42, no. 9, pp. 756-770, 2008.
- [13] Yanqun Jiang, S. C. Wong, H. W. Ho, Peng Zhang, Ruxun Liu and Agachai Sumalee, "A dynamic traffic assignment model for a continuum transportation system", *Trans. Res. Part B: Methodological*, vol. 45, no. 2, pp. 343-363, 2011.
- [14] N. Geroliminis, J. Haddad and M. Ramezani, "Optimal perimeter control for two urban regions with macroscopic fundamental diagrams: A model predictive approach", *IEEE Trans. Int. Transp. Sys.*, vol. 14, pp. 348-359, 2013.
- [15] M. Hajiahmadi, V. L. Knoop, B. De Schutter and H. Hellendoorn, "Optimal dynamic route guidance: A model predictive approach using the macroscopic fundamental diagram", *Intelligent Transportation Systems, 16th Intern. IEEE Conf.*, pp. 1022-1028, 2013.
- [16] J. Haddad, "Robust constrained control of uncertain macroscopic fundamental diagram networks", *Transp. Res. C*, vol. 59, pp. 323-339, 2015.
- [17] F. van Wageningen-Kessels, H. van Lint, K. Vуйk and S. Hoogendoorn, "Genealogy of traffic flow models", *EURO Journal on Transportation and Logistics*, vol. 4, pp. 445-473, 2015.
- [18] Z. Y. Lin, S. C. Wong, P. Zhang, Y. Q. Jiang, K. Choi and Y. C. Du, "A predictive continuum dynamic user-optimal model for a polycentric urban city", *Transportmetrica B: Transport Dynamics*, vol. 5, no. 3, pp. 228-247, 2017.
- [19] S. Mollier, M. L. Delle Monache and C. Canudas-de-Wit, "Two-dimensional macroscopic model for large scale traffic networks", *Transp. Res. Part B: Method.*, vol. 122, pp. 309-326, 2019.
- [20] R. Aghamohammadi and J. A. Laval, "A Continuum Model for Cities Based on the Macroscopic Fundamental Diagram: a Semi-Lagrangian Solution Method", *Trans. Res. Procedia*, vol. 38, pp. 380-400, 2019.
- [21] S. Mollier, M. L. Delle Monache and C. Canudas-de-Wit, "A step towards a multidirectional 2D model for large scale traffic networks", *TRB 2019 - 98th Annual Meeting Transportation Research Board, Washington D.C., USA*, hal-01948466, Jan. 2019.
- [22] R. Aghamohammadi and J. A. Laval, "Dynamic traffic assignment using the macroscopic fundamental diagram: A Review of vehicular and pedestrian flow models", *Transportation Research Part B: Methodological*, vol. 137, pp. 99-118, 2020.
- [23] L. Tumash, C. Canudas-de-Wit and M. L. Delle Monache, "Equilibrium Manifolds in 2D Fluid Traffic Models", *21th IFAC World Congress*, Berlin, Germany, 2020, <https://hal.archives-ouvertes.fr/hal-02513273v2/document>.
- [24] L. Tumash, C. Canudas-de-Wit and M. L. Delle Monache, "Topology-based control design for congested areas in urban networks", *2020 IEEE 23rd International Conference on Intelligent Transportation Systems (ITSC)*, Rhodes, Greece, 2020, pp. 1-6, doi: 10.1109/ITSC45102.2020.9294280.
- [25] L. Tumash, C. Canudas-de-Wit and M. L. Delle Monache, "Boundary and VSL Control for Large-Scale Urban Traffic Networks", submitted to *IEEE Transactions on Automatic Control*, 2021, <https://hal.archives-ouvertes.fr/hal-03167733/document>.
- [26] L. Tumash, C. Canudas-de-Wit and M. L. Delle Monache, "Multi-Directional Continuous Traffic Model For Large-Scale Urban Networks", submitted to *Transportation Research Part B: Methodological*, 2021.